

Advances in Applied Biological Research

Year 2025, Volume-2, Issue-2 (Jul-Dec)



Tinospora cordifolia GCMS profiling and cytotoxic effect on HCT 116- In vitro assay

S. Manimozhi¹ and Dr.V. Sumathi^{2*}

¹. Research scholar, Department of Microbiology, Annamalai University, Chidambaram, Tamil Nadu.

^{2*}. Assistant Professor, Department of Microbiology, Annamalai University, Chidambaram, Tamil Nadu.

ARTICLE INFO

Keywords: Alkaloid, Anticancer, Colon cancer, Antioxidant, Antibacterial

DOI: 10.48165/aabr.2025.2.2.02

ABSTRACT

An assessment of *Tinospora cordifolia* extract's (TCE) antimicrobial and antioxidant properties was undertaken in light of its possible application as cytotoxic against HCT116. Compounds from the stem were Soxhlet extracted with ethyl acetate and identified through GCMS. Antibacterial, antioxidant and HCT cytotoxicity of extract was studied by conventional standard methods. The GC-MS profile highlights a chemically diverse phytochemical composition, with both major and minor compounds potentially responsible for natural antimicrobial and antioxidant agent. The extract has broad spectrum antibacterial activity at concentration dependent manner against both Gram positive and negative clinical pathogens with relative inhibition 83 to 107%. Among the tested antioxidant assay the extract showed the strongest DPPH scavenging with an IC₅₀ value of 12.07 µg/mL, which, although higher than the standard ascorbic acid. Treatment of HCT116 colorectal carcinoma cells with TCE resulted in a dose-dependent reduction in cell viability. Nonlinear regression analysis of the MTT assay revealed an IC₅₀ value of 359 µg/ml, with viability decreasing from ~80% at 300 µg/ml to <10% at 900–1000 µg/ml. Morphological examination and apoptosis assays further confirmed that cell death was predominantly apoptotic nature of cancerous cells. The molecular docking of compounds 2-Fluoro-3-trifluoromethylbenzoic acid found to be strongest binding affinity and non-toxic drug likeness identified as promising new anticancer compound.

INTRODUCTION

Colorectal cancer (CRC) is among the most frequently reported cancers in the globe. CRC is now the second most prevalent cancer diagnosed in women and the third in men, according to Global Cancer Statistics (2018) (Waiet al., 2020). Scientific information on the biological activities and the makeup of the active chemicals in natural plant compounds are still lacking, despite the growing interest in discovering the therapeutic benefits of plants. As a result, scientists look

for various forms of bio activity in plant extracts. *Tinospora cordifolia* also known as Guduchi or Gurjo is regarded as a significant medicinal herb in the Ayurvedic medicinal system. The use of alternative therapies, such as medicinal plants, is therefore very popular. The medicinal effects of natural plant-based products have been the subject of numerous research, particularly in relation to plants found in isolated locations, like the *Tinospora* genus. The only member of the *Tinospora* genus to demonstrate anti-carcinogenic qualities is *Tinospora cordifolia* (Deepa et al., 2019). *Tinospora cordifolia* (Willd.) is

*Corresponding author. Dr.V. Sumathi

E-mail: sumathikarthidd@gmail.com

Copyright @ Advances in Applied Biological Research (<https://acspublisher.com/journals/index.php/aabr/>)

a well-known ayurvedic medicinal herb with different names including *Rasayana* (to purify the blood), *Amrita* (to bring the dead back to life) (Sharma et al., 2019). It is native to the tropical region of India ascending to an altitude of 500 metres in the temperature range of 25 to 45 °C (Tiwari et al., 2018). *Tinospora cordifolia* with great medicinal properties including antioxidants, antimicrobial, anti-diabetic, anti-ageing and cytotoxic activity (Prasad and Hauhan, 2019). *Tinospora cordifolia* is a rich source of bitter alkaloids such as tinosporin, tinosporic acid and tinosporol have been found to exhibit medicinal effects (Singh and Chaudhuri, 2017). *Tinospora cordifolia* has medicinal properties like anti-inflammatory, anti-arthritis, anti-oxidant, hepatoprotective and immunomodulatory activities (Sinha et al., 2017). Berberine (BBR) one of the secondary metabolites this plant has been used to treat cancer against many cell types (Palmieri et al., 2019). Antibacterial activity of *T. cordifolia* extracts of stem are effective against microbial infections against urinary pathogens such as *Klebsiella pneumoniae* and *Pseudomonas aeruginosa* (Shrestha and Lamichhane, 2021). Oxidative stress arises from an imbalance between the body's antioxidant defenses and the creation of reactive oxygen species (ROS). Hence, the exploration of natural antioxidants, such as those present in *Tinospora cordifolia*, holds substantial promise for preventive and therapeutic interventions (Sharma et al., 2024). Therefore, the goal of the current study is to investigate the antibacterial and cytotoxic properties of an ethanol extract of *T. cordifolia* stem using an *in vitro* approach.

MATERIALS AND METHOD

Collection of sample and Extraction process

The Plants belonging to the *Tinospora cordifolia* species are collected in the Cuddalore district (11.679930/79.719829), verified and authenticated at the Department of Botany, Annamalai University, Chidambaram. The plant material stem which had been well-dried and finely ground, was put into a 25 x 80 mm porous cellulose thimble. Ethyl acetate was taken in a round bottom flask then built using a column. The extraction procedure involves heating the setup for 3 h at 50°C on a heating mantle. The watery phase was extracted and then analysed using GCMS.

Antibacterial activity

The ethyl acetate stem extracts of *Tinospora cordifolia* was determined by disk diffusion method (Nyalo et al., 2023) Muller Hinton Agar was prepared and allowed to solidify then spread the test organisms over the media. The 24h old

bacterial culture was swabbed over the agar surface with sterile swab. sterile disk preloaded with *Tinospora cordifolia* at different concentrations such as, 25µg, 50µg, 75 and 100µg. All the sample disk along with standard and negative control were placed over the inoculated plates and then incubated at 37°C for 24 h. The plates were observed for zones of inhibition after 24 h and compared with Gentamycin at a concentration of 10 mg/ml.

$$\text{Eq1. \%RIZD} = (\text{Diameter of test zone} / \text{Diameter of reference zone}) * 100.$$

Antioxidant activity

DPPH assay

The free radicals of the dilute stem extract of *Tinospora cordifolia* was tested using DPPH techniques (1,1-diphenyl-2-picryl hydrazyl). A total of 20 mg of DPPH were dissolved in 20 mL of ethyl acetate for making the stock solution (Tamokou et al., 2012). The assay was performed by Microtiter plate method with final volume of 500µl. 200µl of ethyl acetate, 200µl of DPPH, 100µl of sample at different concentration was added and incubated under dark condition for 5 min. Ascorbic acid is used as the standard. The absorbance was taken at 517 nm. The following formula was used to compute the DPPH scavenging effect of antioxidants.

$$\text{Eq2. Percentage of inhibition} = A_0 - A_1 / A_0 * 100$$

Where, A_0 = The absorbance of control.

A_1 = The absorbance of sample.

Metal chelation assay

Metal chelating activity was measured as described previously, by adding 0.1 mM FeSO₄ (0.2 mL) and 0.25 mM ferrozine (0.4 mL) subsequently into 0.2 mL of test compound in ethyl acetate added at different concentration (Sellal et al., 2019). After incubating at room temperature for 10 min, absorbance of the mixture was recorded at 562 nm. **EDTA used as Standard.** Chelating activity was calculated using the following formula:

$$\text{Eq3. Metal chelating activity} = (A_{\text{control}} - A_{\text{sample}}) / A_{\text{control}} * 100$$

Hydrogen Peroxide Scavenging Activity:

The radical scavenging activity of individual extracts was determined using the H₂O₂ method. Briefly, 2 mL of test solution in ethyl acetate was added to 4.0 mL of H₂O₂ (20 mM) solution in phosphate buffer (pH 7.4) (Hussen and Endalew, 2023). After 10 min, the absorbance was measured at λ_{max} 230 nm against the phosphate buffer blank solution. The percentage scavenging of H₂O₂ was calculated using the equation:

$$\text{Eq4. \% scavenging of H}_2\text{O}_2 = [(A_0 - A_1)/A_0] \times 100,$$

Where,

A₀ = absorbance of the control (phosphate buffer with H₂O₂)

A₁ = absorbance of the test extracts.

MTT assay

Cell culture: Triple Human Colorectal Carcinoma cell line (HCT-116) was obtained from NCCS, Pune. The cells were cultured in Dulbecco's Modified Eagle's Medium (DMEM, HiMedia), supplemented with 10% Fetal Bovine Serum (Gibco), 1% Sodium Bicarbonate, and 1% Sodium pyruvate (HiMedia). The cells were maintained in a humidified 5% CO₂ atmosphere at 37°C for further experiments.

Cytotoxicity analysis by MTT:

MTT (Tetrazolium salt; HiMedia) was used to analyze the effective cytotoxic concentration of the Sample Drug. HCT116 cells were seeded (1×10⁴ cells per well) in a 96-well plate (Ungureanu *et al.*, 2023). The cells were then incubated for 24 hours. Cells were treated with a Sample Drug (Crude Extract at 100 - 1000 µg/ml concentration), and incubated for another 24 hours. 100µl of complete media containing MTT (0.5mg/ml) was added to each well, the cells were incubated for 5 hours, the media was carefully removed, and the formazan crystals were dissolved in 100µl DMSO for 30 minutes. The absorbance was then obtained on a microplate reader at 570 nm and 650 nm, and the IC₅₀ value was calculated.

Platform for molecular docking

Protein preparation

The molecular docking technique was utilized to comprehend the binding interaction of the NIST matched compound

against CDK4 (PDB ID:7SJ3). The unwanted co-crystallized ligand and water molecules were removed and the enzyme was prepared using the QuickPrep tool module in the MOE program, saved as pdb and converted to PDBQT format by Autodock vina. AutoDock Tools was employed to set the size and the centre of the grid box. Partially charged atoms were allocated partial charges, and polar hydrogen was added to create a protonation state at physiological pH.

Ligand preparation

All constituents' three-dimensional (3D) structures were obtained from the PubChem database, which is accessible via the NCBI website (<https://pubchem.ncbi.nlm.nih.gov/>), using the UCSF Chimera program (v.1.14).

Molecular docking

To forecast the ligand molecules binding affinity, molecular docking assesses the interactions between proteins and ligands and calculates the scoring function based on geometry. The AutoDock Vina feature in the UCSF Chimera program version 1.14 was utilized to carry out the molecular docking study (Butt *et al.*, 2022). View Dock was used to investigate binding affinity. Using Discovery Studio 2020 Client, the final results were examined and displayed.

Absorption, distribution, metabolism, and excretion (ADME) and toxicity prediction

Lipinski's rule was used to further examine the phytoconstituents that were chosen for their potential as drugs. With the use of Swiss ADME, ligand pharmacokinetic profile (ADME) (Ononamadu and Ibrahim, 2021). and toxicity predictions were performed. Uploading SDF files or Simplified Molecular Input Line Entry System (SMILES) notations allowed for the analysis of the toxicological characteristics of ligands.

RESULTS AND DISCUSSION

Compound analysis of ethyl acetate extract

GC-MS analysis of the extract revealed the presence of diverse bioactive compounds, as summarized in (Table 1). A total of 20 peaks were identified, corresponding to compounds belonging to different classes, including organic acids, esters, siloxanes, heterocycles, and complex bicyclic

derivatives (Figure 1). The most abundant component was Hexanedioic acid, bis(2-ethylhexyl) ester (39.59% peak area; RT 32.884 min), a phthalate derivative commonly reported as a plasticizer but also associated with antimicrobial and antioxidant properties. Other major constituents included Cyclohexasiloxane, dodecamethyl- (11.38%; RT 13.876 min), 1,2-Benzenedicarboxylic acid, dicyclohexyl ester (9.70%; RT 24.844 min), and 1,3-diphenyl-1-((trimethylsilyl)oxy)-1(Z)-heptene (5.69%; RT 17.486 min). Minor compounds such as 2-keto-butyrac acid (1.28%; RT 6.83 min), benzoic acid derivatives (2.45%; RT 9.958 min), nonanoic acid methyl ester (3.63–3.53%), and 2(E)-tert-butyladamantan-2,4-diol (2.83%) contribute to the biochemical complexity of the extract. Several nitrogen- and oxygen-containing heterocyclic compounds, including Furo[2,3-c] pyridine,

2,3-dihydro-2,7-dimethyl- and 12-azabicyclo (9.2.1) tetradeca-1(14)-ene-13-one (multiple peaks, total >5%), were also detected, indicating the presence of alkaloid-like structures. The presence of phthalate esters and siloxane derivatives, while sometimes considered contaminants, compounds such as benzoic acid derivatives, nonanoic acid esters, and phthalates have been widely documented for their antibacterial, antifungal, and antioxidant activities, which correlate with the observed bioassays of the extract (Chi *et al.*, 2016). In particular, the detection of esters like hexanedioic acid bis(2-ethylhexyl) ester and aromatic derivatives suggests that these metabolites may contribute synergistically to the extract's antimicrobial and free radical scavenging potential (Sowmya *et al.*, 2024).

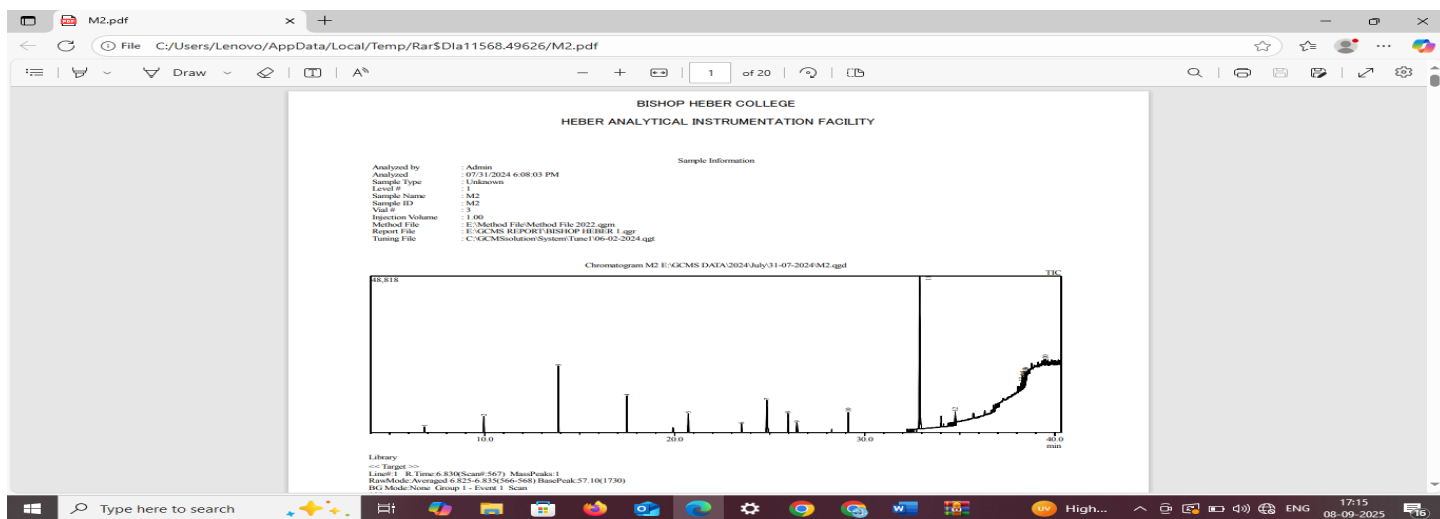


Figure 1. Retention time of peaks eluted from Ethyl acetate extract

Table 1. Compounds identified from GCMS spectrum

Peak	Retention time	Area %	Name
1	6.83	1.28	2-Keto-butyrac acid
2	9.958	2.45	Benzoic acid, 2,6-bis(trimethylsiloxy)-, trimethylsilyl ester
3	13.876	11.38	Cyclohexasiloxane, dodecamethyl-
4	17.486	5.69	1,3-Diphenyl-1-((trimethylsilyl)oxy)-1(z)-heptene
5	20.718	2.99	Tri-o-trimethylsilyl, n-trifluoroacetyl derivative of terbutaline
6	23.512	0.98	Phosphonous dibromide, [2,2,2-trifluoro-1-(trifluoromethyl)-1-[(trimethylsilyl)oxy]ethyl]-
7	24.844	9.7	1,2-Benzenedicarboxylic acid, dicyclohexyl ester
8	25.955	3.63	Nonanoic acid, methyl ester
9	26.43	2.25	Furo[2,3-c]pyridine, 2,3-dihydro-2,7-dimethyl-
10	29.132	3.53	Nonanoic acid, methyl ester
11	32.884	39.59	Hexanedioic acid, bis(2-ethylhexyl) ester
12	34.76	2.83	2(E)-Tert-butyladamantan-2(a),4(a)-diol
13	38.255	2.69	1-Hydroxyspiro[5.12]octadecan-7-one
14	38.295	2.63	2-(N-Methylpyrrolyl) furoate
15	38.35	1.07	12-Azabicyclo(9.2.1)tetradeca-1(14)-ene-13-one

16	38.381	1.22	1,5,7-Trimethyl-3-oxo-2-oxabicyclo[4.2.0]oct-4-ene-(endo)-7-carbonitrile
17	38.405	1.33	2-Fluoro-3-trifluoromethylbenzoic acid, heptyl ester
18	38.44	2.45	12-Azabicyclo(9.2.1)tetradeca-1(14)-ene-13-one
19	38.491	1.79	12-Azabicyclo(9.2.1)tetradeca-1(14)-ene-13-one
20	39.507	0.51	Cesium trimethylfluoro) aluminate

Antioxidant potential of TC extract

The antioxidant potential of the extract was assessed using hydroxyl radical scavenging, DPPH radical scavenging, and metal chelation assays at concentrations ranging from 25–100 µg/mL (Table 2). Hydroxyl radical scavenging activity increased in a dose-dependent manner, from 33.00 ± 1.00% at 25 µg/mL to 72.00 ± 1.00% at 100 µg/mL, with an IC₅₀ value of 331.97 µg/mL. DPPH radical scavenging activity was markedly higher, with inhibition values of 62.04 ± 0.00% at 25 µg/mL and 82.31 ± 0.00% at 100 µg/mL, yielding a comparatively lower IC₅₀ of 12.078 µg/mL. In the metal chelation assay, the extract exhibited moderate chelating ability, ranging from 39.69 ± 1.00% at 25 µg/mL to 64.16 ± 0.32% at 100 µg/mL with an IC₅₀ value of 67.86 µg/mL. These results indicate that the extract exerts considerable antioxidant activity, particularly through DPPH radical scavenging.

In comparison with standard antioxidants, the extract's DPPH scavenging potential is noteworthy. While its IC₅₀

(67.86 µg/mL) was higher than that of ascorbic acid (5–20 µg/mL, as reported in earlier studies), the strong dose-dependent inhibition highlights the presence of efficient free radical quenchers such as phenolics and flavonoids. Hydroxyl radical scavenging was relatively less potent (IC₅₀: 331.97 µg/mL), suggesting that while the extract can neutralize highly reactive hydroxyl radicals, it is not as effective as pure standards. Metal chelation activity was moderate, reaching 64.16% at 100 µg/mL, but remained lower than EDTA, which typically achieves >90% chelation at equivalent concentrations. The observed activity may be attributed to secondary metabolites such as tannins and polyphenolic compounds, which possess hydroxyl and carbonyl groups capable of binding metal ions. *Tinospora cordifolia aqueous* extract reported as better antioxidative properties than solvent by (Boro *et al.*, 2025). Likewise (Polu *et al.*, 2017) have stated that ethanol extract and n-butanol fractions found to be superior radical scavenging in DPPH and metal chelation.

Table 2. Antioxidant activity of Ethyl acetate extract

Con.	OH Scavenging	SD	DPPH	SD	Metal chelation	SD
25	33	1	62.04	0	39.69	1.004
50	47.66	0.57735	77.30	0.34	41.77	5.046
75	55.33	0.57735	80.62	0	57.31	1.059
100	72	1	82.31	0	64.16	0.321
IC ₅₀ µg	331.97		12.078		67.867	

Antibacterial activity

The antibacterial activity of the extract was evaluated against seven bacterial pathogens and compared with a standard antibiotic (Table 3). The extract exhibited broad-spectrum inhibitory effects with zones of inhibition ranging from 19.33 ± 0.57 mm to 21.66 ± 1.52 mm. The maximum inhibition was observed against *Klebsiella pneumoniae* (21.66 ± 1.52 mm), followed closely by *Proteus mirabilis* (21.33 ± 1.15 mm) and *Pseudomonas aeruginosa* (20.66 ± 0.57 mm). Significant activity was noted against *Escherichia coli* (20.33 ± 1.52 mm), *Enterococcus faecalis* (20.00 ± 1.00 mm), and *Staphylococcus aureus* (19.33 ± 0.57 mm). Interestingly, the extract displayed greater activity against *Bacillus sp.* (19.33 ± 1.15 mm) compared to the standard drug (18.00 ± 0.00 mm), indicating selective potency. Although the standard

antibiotic consistently produced slightly larger inhibition zones, the extract demonstrated significant and reliable antibacterial activity. No inhibition was observed with the negative control, confirming that the activity was solely attributable to the extract. The data found to be similar to the report of (Kumar *et al.*, 2017). It was also reported that *Tinospora cordifolia* plays a potential role in combating the drug resistance among clinical pathogens (Ezhilarasu *et al.*, 2023). The relative inhibitory zone diameter (RIZD) analysis revealed that the extract exhibited potent antibacterial activity against all tested organisms, with values ranging from 83.11% to 107.47% of the standard (Figure 2). The highest relative activity was recorded against *Bacillus sp.* (107.40%), where the extract outperformed the standard antibiotic. Strong inhibitory effects were also observed against *Staphylococcus aureus* (95.08%), *Pseudomonas aeruginosa* (96.87%), and

Enterococcus faecalis (88.23%). Moderate relative activity was noted against *Escherichia coli* (87.14%), *Klebsiella pneumoniae* (85.52%), and *Proteus mirabilis* (83.11%). These findings confirm that the extract possesses broad-spectrum antibacterial activity, in some cases surpassing the standard drug.

Table 3. Antibacterial activity of ethyl acetate extract

Organisms	Extract Zone		Standard Zone		NC
	(mm)	SD	(mm)	SD	
<i>K.pneumoniae</i>	21.66	1.52	25.33	1.15	0
<i>P.mirabilis</i>	21.33	1.15	25.66	0.57	0
<i>S.aureus</i>	19.33	0.57	20.33	0.57	0
<i>E.faecalis</i>	20	1	22.66	1.15	0
<i>P.aeruginosa</i>	0.57		21.33		0
<i>E.coli</i>	20.33	1.52	23.33	1.15	0
<i>Bacillus sp</i>	19.33	1.15	18	0	0

exhibit membrane blebbing, cell shrinkage, and chromatin condensation, which are hallmark features of apoptosis. Detached, rounded cells and apoptotic bodies are visible compared to the intact morphology of control cells (Image 1). Necrotic cells are relatively few, suggesting cell death is mainly apoptotic rather than necrotic. The results are concurrent with the findings of (Patil et al., 2021) who have reported cytotoxic effect of *Tinospora cordifolia* on Oral colon cell. (Ali and Dixit, 2013) reported the anticancer activity of alkaloid palmatine derived from *Tinospora cordifolia*

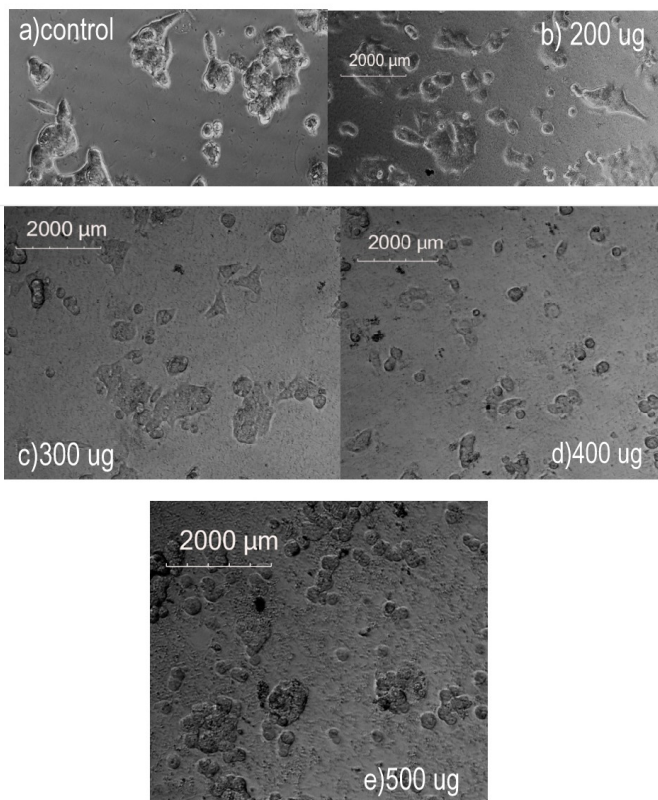


Image 1. Microscopic observation of HCT 116 cell proliferation inhibition by MTT assay

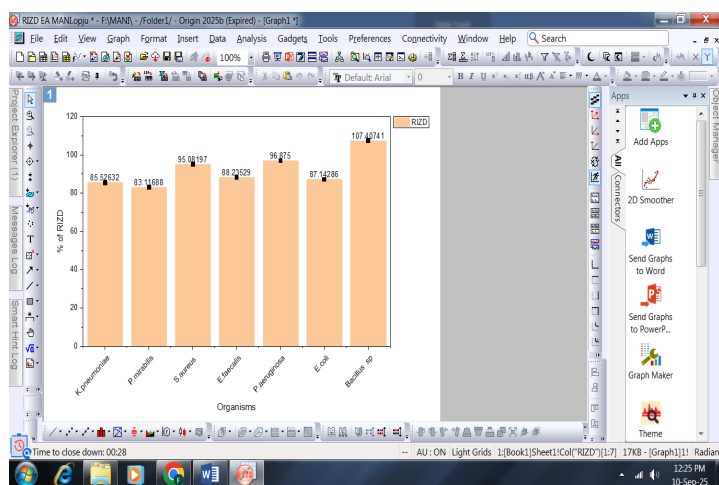


Figure 2. Percentage of relative inhibition by extract

Cytotoxic effect of extract on HCT116

Figure 3(a) represents the cytotoxicity curve for HCT116 cells treated with compound extract at different concentrations (100–1000 µg/ml). The y-axis shows % cell viability, and the x-axis shows drug concentration. At ~300 µg/ml, viability is about 75–80%. At ~400 µg/ml, viability drops sharply to around 25–30%. At 500 µg/ml, viability is ~20%. The IC₅₀ (half-maximal inhibitory concentration) is the concentration where 50% cell viability remains was recorded from does response curve and calculated ad 359 µg/ml [Fig 3 (b)]. Compound M induces apoptosis in HCT116 cells in a dose-dependent manner, with the majority of cell death attributable to programmed cell death rather than necrosis. This aligns with cytotoxicity data (IC₅₀ ≈ 359 µg/ml), showing a strong apoptotic mechanism at higher concentrations. Cells

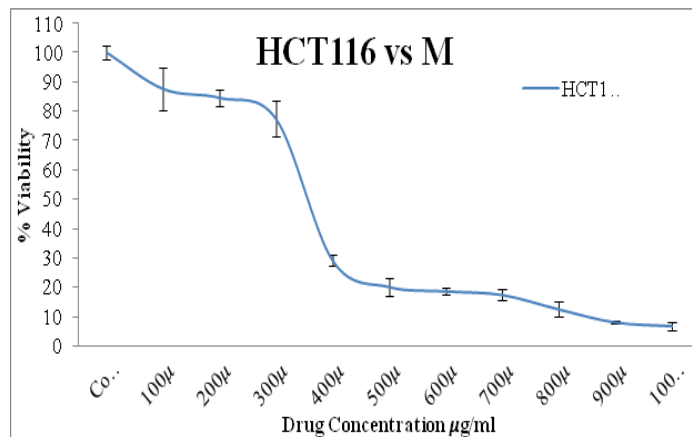


Figure 3 (a). HCT116 cell viability among different concentration of extract

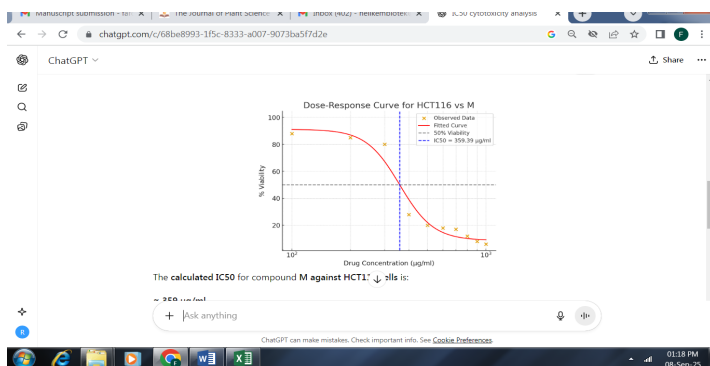


Figure 3(b). Dose response curve on HCT116 cytotoxicity

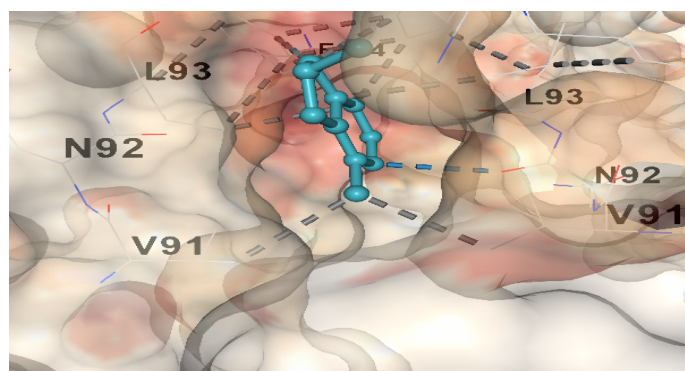
In silico analysis of active compound

The ADME/T profile of selected GC-MS identified compounds was evaluated to assess their drug-likeness and pharmacokinetic properties (Table 4). *Furo[2,3-c] pyridine, 2,3-dihydro-2,7-dimethyl-* exhibited a molecular weight of 149.08 Da, good solubility ($\log S = -1.417$), moderate lipophilicity ($\log P = 1.77$), and complete blood-brain barrier (BBB) penetration (1.0). In contrast, *2-Fluoro-3-trifluoromethylbenzoic acid, heptyl ester* was heavier (306.12 Da), less soluble ($\log S = -5.941$), and more lipophilic ($\log P = 5.182$), with partial BBB penetration (0.799). Both compounds satisfied Lipinski's rule of five, indicating acceptable oral bioavailability. Regarding absorption and distribution, both compounds showed low predicted human intestinal absorption ($HIA = 0.0-0.001$), but high plasma protein binding (PPB: 75.84% and 99.23%), which suggests strong binding affinity in systemic circulation. Both were predicted as P-glycoprotein substrates, although with low probabilities, indicating possible efflux by Pgp transporters. Metabolism predictions indicated that both molecules may act as CYP1A2 inhibitors, while *2-Fluoro-3-trifluoromethylbenzoic acid, heptyl ester* additionally inhibited CYP2C19. These interactions suggest potential influence on hepatic drug metabolism. Both compounds were predicted to undergo clearance (CL = Yes) and exhibit extended half-life ($T_{1/2} = \text{Yes}$).

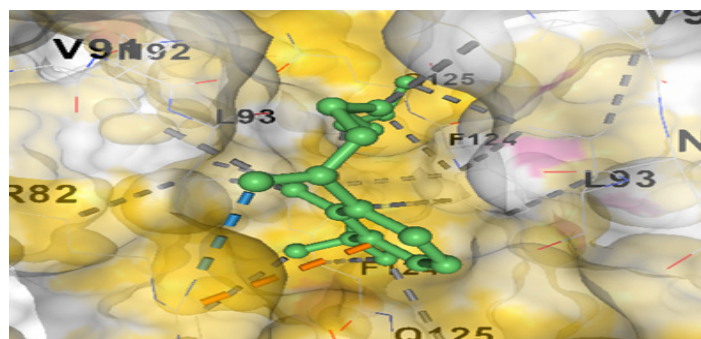
Toxicity profiling indicated mixed results on *Furo[2,3-c] pyridine* tested positive for Ames mutagenicity, hepatotoxicity, acute oral toxicity, and carcinogenicity, whereas the heptyl ester derivative was non-mutagenic, non-carcinogenic, and showed lower acute oral toxicity risk, though hepatotoxic potential remained. Overall, *Furo[2,3-c] pyridine* demonstrated favorable physicochemical and BBB penetration properties but with concerning mutagenic and carcinogenic predictions. *2-Fluoro-3-trifluoromethylbenzoic acid, heptyl ester* displayed better drug-likeness, non-mutagenicity, and non-carcinogenicity, although high plasma protein binding and CYP inhibition may limit its pharmacological safety. These findings suggest that while both compounds may contribute to the extract's bioactivity,

careful consideration of toxicity is essential before therapeutic applications.

Furo[2,3-c] pyridine, 2,3-dihydro-2,7-dimethyl interaction with target protein was represented on [Figure 4 (a)]. The cavity volume of the binding for 2A25, its 1263 \AA^3 . Binding score (in kcal/mol) was -5.5 indicates moderate binding affinity (more negative usually means stronger predicted binding). Lists residues forming hydrogen bonds with the ligand was ASN, VAL, LEU, and PHE. Residues involved in hydrophobic or van der Waals interactions. *2-Fluoro-3-trifluoromethylbenzoic acid, heptyl ester* interaction with target protein was represented on [Figure 4(b)]. The cavity volume of the binding for 2A25, its 1263 \AA^3 . The docking score (here, -6.9) is an estimate of the binding affinity (Table 5). More negative values generally indicate stronger predicted binding between the ligand and the protein. Lists residues involved in hydrogen bonding with the ligand was ARG, VAL, 2LEU, GLN, PHE Residues involved in hydrophobic or van der Waals interactions. Previously series of furopyridine (PD) compounds were virtually screened to identify potent EGFR inhibitors using molecular docking (Todsaporn *et al.*, 2024) likewise (Ren *et al.*, 2024) synthesized Furopyridone derivatives as cytotoxic agents against esophageal Cancer. Literature states that anticancer compounds like 4-Fluoro-2-trifluoromethylbenzoic acid identified from *Callistemon lanceolatus* leaves (Ahmad *et al.*, 2018).



(a) Furo [2,3-c] pyridine



(b) 2-Fluoro-3-trifluoromethylbenzoic acid

Figure 4. Interaction of ligands with CDK4

Table 4. ADMET of compounds selected from GCMS

S.NO	COMPOUND NAME	Furo[2,3-c]pyridine, 2,3-dihydro-2,7-dimethyl-	2-Fluoro-3-trifluoromethylbenzoic acid, heptyl ester
1	Molecular Weight	149.08	306.12
2	nHA	2.0	2.0
3	nHD	0.0	0.0
4	logS	-1.417	-5.941
5	logP	1.77	5.182
6	HIA	0.0	0.001
7	BBB Penetration	1.0	0.799
8	Pgp-substrate	0.019	0.01
9	Lipinski Rule	0.0	0.0
10	F20%	0.002	0.067
11	PPB	75.841	99.239
12	CYP1A2 inhibitor	Yes	Yes
13	CYP2C19 inhibitor	No	Yes
14	CL	Yes	Yes
15	T1/2	Yes	Yes
16	AMES Toxicity	Yes	No
17	Hepatotoxicity	Yes	Yes
18	Rat Oral Acute Toxicity	Yes	No
19	Carcinogenicity	Yes	No

Table 5. Binding affinity of active compounds identified from extract

COMPOUND	CV(Å ³)	SCORE	H BOND	OTHER
Furo [2, 3-c] pyridine, 2, 3-dihydro-2, 7-dimethyl-	1263	-5.5	ASN	VAL, LEU, PHE
2-Fluoro-3-trifluoromethylbenzoic acid, heptyl ester	1263	-6.9	ARG	VAL, 2LEU, GLN, PHE

Conclusion

The results show that the extract has broad spectrum antibacterial and wide range of antioxidant processes, such as metal ion chelation and free radical scavenging. These findings imply that the extract exhibited antiproliferation of cancerous cells promising as anticancer agent that causes concentration-specific apoptosis in HCT116 cells. Further studies on the extract may also be investigated in future for the treatment of potentially malignant conditions under *in vivo* to confirm its ability to prevent cancer.

REFERENCE

- Ahmad, K., Hafeez, Z.B., Bhat, A.R., Rizvi, M.A., Thakur, S.C., Azam, A. and Athar, F. 2018. Antioxidant and apoptotic effects of *Callistemon lanceolatus* leaves and their compounds against human cancer cells. *Biomed Pharmacother*, 106:1195-1209
- Ali, H. and Dixit, S. 2013. Extraction optimization of *Tinospora cordifolia* and assessment of the anticancer activity of its alkaloid palmatine. *Sci. World J.* 1–10.
- Boro, A., Sujatha, K., Abidharini, J.D., Pallavi, P., Prabhu, J.P.A. and Anand, A.V. 2025. Evaluation of the Antioxidative and Qualitative Properties of the *Tinospora cordifolia*. *Free Radicals and Antioxidants*, 14:2, 126–130.
- Butt, S.S., Badshah, Y., Shabbir, M. and Rafiq, M. 2022. Molecular Docking Using Chimera and Autodock Vina Software for Nonbioinformaticians. *JMIR Bioinform Biotech* 2020;1(1): e14232.
- Chi, S., She, G., Han, D., Wang, W., Liu, Z. and Liu, B. 2016. Genus *Tinospora*: Ethnopharmacology, Phytochemistry, and Pharmacology. *Evidence-based complementary and alternative medicine*, Article ID 9232593.
- Deepa, B., Babaji, H.V., Hosmani, J. V., Alamir, A. W. H., Mushtaq, S., Raj, A. T. and Patil, S. 2019. Effect of *Tinospora cordifolia*-

- Derived Phytochemicals on Cancer: A Systematic Review. *Applied Sciences*, 9: 23, 5147.
- Ezhilarasu, K., Kasiranjani, A., Priya, S. and Kamaraj, A. 2023. The Antibacterial Effect of *Tinospora Cordifolia* (Guduchi) and Its Role in Combating Antimicrobial Resistance. *Medeni Med J*, 38(3):149-158.
- Hussen, E.M., and Endalew, S.A. 2023. *In vitro* antioxidant and free-radical scavenging activities of polar leaf extracts of *Vernonia amygdalina*. *BMC Complement Med Ther* 23, 146.
- Kumar, DV., Geethanjali, B., Avinash, K.O., Kumar, J.R., Chandrashekrappa, G.K. and Basalingappa K.M. 2017. *Tinospora cordifolia*: The antimicrobial property of the leaves of Amruthaballi. *JBMOA*, 5:147-56
- Nyalo, P. O., Omwenga, G. I. and Ngugi, M. P. 2023. Antibacterial properties and GC-MS analysis of ethyl acetate extracts of *Xerophyta spekei* (Baker) and *Grewia tembensis* (Fresen). *Heliyon*, 9(3), e14461.
- Ononamadu, C. J. and Ibrahim, A. 2021. Molecular docking and prediction of ADME/drug-likeness properties of potentially active antidiabetic compounds isolated from aqueous-methanol extracts of *Gymnema sylvestre* and *Combretum micranthum*. *Biotechnology*, 102(1), 85-99.
- Palmieri, A., Scapoli, L., Iapichino, A., Mercolini, L., Mandrone, M., Poli, F., Gianni, A. B., Baserga, C. and Martinelli, M. 2019. Berberine and *Tinospora cordifolia* exert a potential anticancer effect on colon cancer cells by acting on specific pathways. *International journal of immunopathology and pharmacology*, 33, 2058738419855567.
- Patil, S., Ashi, H., Hosmani, J., Almalki, A.Y., Alhazmi, Y.A., Mushtaq, S., Parveen, S., Baeshen H.A, Varadarajan, S., Raj, A.T., Patil, V.R. and Vyas, N. 2021. *Tinospora cordifolia* (Thunb.) Miers (Giloy) inhibits oral cancer cells in a dose-dependent manner by inducing apoptosis and attenuating epithelial-mesenchymal transition. *Saudi J Biol Sci*, 28(8):4553-4559.
- Polu, P.R., Nayanbhirama, U., Khan, S. and Maheswari R. 2017. Assessment of free radical scavenging and anti-proliferative activities of *Tinospora cordifolia* Miers (Willd). *BMC Complement Altern Med*, 17(1):457.
- Prasad, B., and Chauhan, A. 2019. Anti-oxidant and antimicrobial studies of *Tinospora cordifolia* (Guduchi/Giloy) stems and roots under *in-vitro* condition. *Int J Adv Microbiol Health Res*, 3(1), 1-10.
- [Ren, X., Zhang, J., Dai, A., Sun, P., Zhang, Y., Jin, L. and Pan, L. 2024. Synthesis and Biological Evaluation of Novel Furopyridone Derivatives as Potent Cytotoxic Agents against Esophageal Cancer. *International Journal of Molecular Sciences*, 25\(17\):9634.](#)
- Sellal, A., Belattar, R. and Bouzidi, A. 2019. Heavy Metals Chelating Ability and Antioxidant Activity of *Phragmites australis* Stems Extracts. *Journal of Ecological Engineering*, 20(2), 116-123.
- Sharma, B., Yadav, A., and Dabur, R. 2019. Interactions of a medicinal climber *Tinospora cordifolia* with supportive interspecific plants trigger the modulation in its secondary metabolic profiles. *Scientific Reports*, 9, 14327.
- Sharma, S., Mehmood, Y., Sharma, V., Kumar, A., Kumar, S. and Bhat, Z. 2024. Antioxidant potential of *Tinospora cordifolia*: Insights into its therapeutic significance. *International Journal of Advanced Biochemistry Research*, 8(2), 425-427.
- Shrestha, T., and Lamichhane, J. 2021. Assessment of phytochemicals, antimicrobial, antioxidant and cytotoxicity activity of methanolic extract of *Tinospora cordifolia* (Gurjo). *Nepal Journal of Biotechnology*, 9(1), 18-23.
- Singh, D. and Chaudhuri, P. K. 2017. Chemistry and pharmacology of *Tinospora cordifolia*. *Natural product communications*, 12(2), 1934578X1701200240.
- Sinha, A., Sharma, H., Singh, B. and Patnaik, A. 2017. Phytochemical studies of methanol extracts of *Tinospora cordifolia* stem by Gc-MS. *World Journal of Pharmaceutical Research*, 6(4), 1319-1326.
- Sowmya, M., Ramesh, S., Ganne Venkata Sudhakar Rao, Ramesh, S., Jalandha, P., Sujatha, P. L. and Indumathi. R. 2024. Phytochemical Analysis of *Tinospora Cordifolia* by Gc-MS and Evaluation of its Antiuro lithiatic Potential by *In Silico*. *The Indian Veterinary Journal*, 101(4), 39-48.
- Tamokou, J.deD., Simo Mpetga, D. J., Keilah Lunga, P., Tene, M., Tane, P. and Kuate, J. R. 2012. Antioxidant and antimicrobial activities of ethyl acetate extract, fractions and compounds from stem bark of *Albizia adianthifolia* (Mimosoideae). *BMC complementary and alternative medicine*, 12, 99.
- Tiwari, P., Nayak, P., Prusty, S. K., and Sahu, P. K. 2018. Phytochemistry and pharmacology of *Tinospora cordifolia*: A review. *Systematic Reviews in Pharmacy*, 9 (1), 70-78.
- Todsaporn, D., Zubenko, A., Kartsev, V. G., Mahalapbutr, P., Geronikaki, A., Sirakanyan, S. N., Divaeva, L. N., Chekrisheva, V., Yildiz, I., Choowongkamon, K. and Rungrotmongkol, T. 2024. Furopyridine Derivatives as Potent Inhibitors of the Wild Type, L858R/T790M, and L858R/T790M/C797S EGFR. *The journal of physical chemistry. B*, 128 (50), 12389-12402.
- Ungureanu, A. R., Popovici, V., Oprean, C., Danciu, C., Schroder, V., Olaru, O. T., Mihai, D. P., Popescu, L., Luta, E. A., Chitescu, C. L. and Gird, C. E. 2023. Cytotoxicity Analysis and *In Silico* Studies of Three Plant Extracts with Potential Application in Treatment of *Endothelial Dysfunction*. *Pharmaceutics*, 15(8), 2125.
- Wai Hon, K., Zainal Abidin, S. A., Othman, I. and Naidu, R. 2020. Insights into the Role of microRNAs in Colorectal Cancer (CRC) Metabolism. *Cancers*, 12 (9), 2462.